

L-shell ionization of Si, P, S, Cl, and Ar by 0.4–2.1-MeV He⁺ bombardment

W. M. Ariyasinghe and D. Powers

Department of Physics, Baylor University, Waco, Texas 76798

(Received 27 November 1989; revised manuscript received 18 January 1990)

The *L*-shell ionization cross sections of Si, P, S, Cl, and Ar have been obtained for incident He⁺ ion energies 0.4–2.1 MeV in steps of 0.2 MeV. The cross sections were obtained from the Auger electron yields measured for SiH₄, PH₃, H₂S, CH₃Cl, and Ar gaseous targets. The present experimental *L*-shell ionization cross sections are compared to existing experimental *L*-shell ionization cross sections as well as to previous theoretical predictions.

I. INTRODUCTION

Inner-shell ionization of atoms by charged particles has been a subject of continuing interest for the past two decades.^{1–11} Considerable efforts, both experimental and theoretical, have been carried out and remarkable progress has been made in understanding the charged-particle, atomic-collision process. The theoretical and experimental *K*-shell ionization cross sections^{2–5} for MeV protons and He⁺ ions agree fairly well for target elements $Z_2 \geq 4$, but similar agreement for *L*-shell ionization cross sections is found only for $Z_2 \geq 18$.^{1,6} Brandt and Lapicki¹ have pointed out that the sparsely available experimental *L*-shell ionization cross sections for third-row elements Mg, Al, S, and Cl are in disagreement with the existing theories, and that the need exists to extend the experimental measurements for these elements to a wide range of projectile energies and also to the additional elements Si and P.

Since an inner-shell ionized atom will undergo x-ray or Auger-electron emission, the ionization mechanism may be studied by measuring either of these processes. The experimental x-ray or Auger yields, along with calculated fluorescence and Coster-Kronig yields,¹² may be used to find the ionization cross sections. Since *L*-shell x rays for third-row elements have energy of only 20 to 240 eV, it is essential to have a detector that can register the soft x rays efficiently. Alternatively, since the *L*-shell fluorescence yields¹² are lower than 10^{-3} for third-row elements, the effect of radiation emission in *L*-shell ionization may be neglected, and the Auger electron yields may be used to determine the ionization cross sections. A commercial spherical-sector electrostatic analyzer of the type employed in the present experiment provides a sufficient means for obtaining *LMM* Auger electron spectra with adequate counting rates (several thousand counts per energy interval per hour) and with good energy resolution (0.45 eV or better).

The *L*-shell ionization cross section of Ar ($Z_2 = 18$) has been studied experimentally by several authors^{7,9,13,14} for a wide range of proton and He⁺ ion energies from 100 keV to 2.5 MeV. These experimental cross sections are in fair agreement with energy-loss Coulomb-deflection perturbed-stationary-state relativistic (ECPSSR) theoretic

cal predictions. Maeda *et al.*¹³ have reported the *L*-shell ionization cross sections for Cl ($Z_2 = 17$) in gaseous CCl₂F₂ by measuring with a channeltron detector the *LMM* Auger yield of Cl under 0.46–2.6-MeV proton and He⁺ ion bombardment, but Brandt and Lapicki¹ found these measurements to be well above the ECPSSR and relativistic plane-wave Born approximation (PWBAR) theoretical predictions by as much as 64% and 82%, respectively. On the other hand, the experimental *L*-shell ionization cross-section measurements for sulfur ($Z_2 = 16$) in gaseous SF₆ for 0.3 to 1.8-MeV protons by Toburen *et al.*¹⁵ fall well below the same theoretical predictions by as much as 60%. The only other *L*-shell ionization cross section measurements for third-row elements are those by Benazeth *et al.*¹⁶ for Mg and Al under 10- to 100-keV He⁺ ion bombardment, and are higher than the binary-encounter approximation (BEA) theory of Gerjuoy¹⁷ by 0% at 100 keV to 2000% at 10 keV for Mg and by 0% at 100 keV to 450% at 10 keV for Al.

In the present experiment, *LMM* Auger yields of third-row elements Si, P, S, Cl, and Ar are measured for 0.4–2.1-MeV He⁺ ions. The total *L*-shell ionization cross sections are then determined from these Auger yields and are compared to the ECPSSR and PWBAR theories as well as to existing experimental *L*-shell ionization cross sections. No previous measurements exist for *LMM* Auger yields and *L*-shell ionization cross sections for Si and P under MeV He⁺ or proton bombardment, or for *L*-shell ionization cross sections of S under MeV He⁺ ion bombardment. The measurements in the present experiment are made by use of gaseous molecular compounds of Si (silane SiH₄), P (phosphine PH₃), S (hydrogen sulfide H₂S), Cl (methyl chloride CH₃Cl), and also for atomic argon gas ($Z_2 = 18$) as a reference standard throughout the course of the other measurements.

II. EXPERIMENT

A detailed description of the experimental procedure will be given here since several modifications have been made to the original equipment^{18,19} used previously to measure Auger electron cross sections. 0.4–2.0-MeV He⁺ ions from a Van de Graaff accelerator were magnetically analyzed and directed through a small 6-cm-long

rectangular-shaped differentially pumped gas cell (with open end windows) mounted perpendicular to and centered on the axis of an 18-in.-diam soft-iron cylindrical scattering chamber whose inside configuration was shielded with μ -metal to eliminate external magnetic fields. The entrance aperture to the gas cell is 1 mm in diameter and the exit aperture is 1.2 mm. An electron trap, biased to -425 V, was located between the entrance port to the scattering chamber and the gas cell to prevent any secondary electrons carried by the He^+ ion beam from reaching the gas cell. The ion beam current, typically 100 nA, was collected in a Faraday cup. The residual vacuum in the scattering chamber was maintained by a Leybold-Heraeus Turbovac Turbomolecular Pump (Model TMP 360) in the low 10^{-6} -Torr region.

Research-grade gases of Ar, CH_3Cl , H_2S , and SiH_4 from Matheson Co., Laporte, Texas, and PH_3 from Liquid Air Corp., Denver, Colorado, all with minimum purities of 99.5% or better, were admitted through a gas transport system into the gas cell where they came to equilibrium at pressures, typically 3 mTorr, as measured with a calibrated Varian Model 531 Thermocouple Gauge. The purities of the gases were confirmed by an Ametek residual gas analyzer (RGA), Model MA 100, which was mounted directly on the cylindrical wall of the scattering chamber. The RGA also gave an independent check throughout the experiment that no air or other gas contamination was leaking into the system through the target gas supply system. A 1-mm-diam hole in the gas cell allowed Auger electrons produced at the center of the gas cell to exit the gas cell in a horizontal plane and at 90° to the He^+ ion beam direction. A 160° spherical sector electrostatic analyzer (ESA) from Comstock, Inc., Oak Ridge, Tennessee, operated in constant energy (30-eV) transmission mode with 0.45-eV resolution or better, was mounted with its radial configuration in a vertical plane passing through the vertical axis of the scattering chamber so that the Auger electrons from the gas cell were electrostatically deflected through the ESA onto two microchannel plates (MCP), Model VUW-8960ES, from Varian Associates, Palo Alto, California, positioned in chevron configuration. Retarding ramp voltages of -35 to -145 V (Si), -45 to -155 V (P), -65 to -175 V (S), -90 to -200 V (Cl), and -120 to -230 V (Ar) were used on the ESA to acquire the Auger spectra, which were collected in an EG&G Ortec Model 7150 Multichannel Analyzer (MCA). The ramp voltages were selected to ensure that each Auger spectrum was collected in the middle portion of the MCA viewing screen with sufficient overlap at the low- and high-energy portions of the spectrum to allow for meaningful background subtraction.

The lowest energy Auger electrons detected by the MCP were 50 eV (Si), 65 eV (P), 110 eV (S), 135 eV (Cl), and 160 eV (Ar), which correspond to MCP efficiencies of 50% (Si) to 68% (Ar).²⁰⁻²² A correction must, therefore, be made to account for the decrease in MCP efficiency. The procedure used to make this correction was to find the mean Auger energy for each spectrum $(\sum_i n_i E_i)/(\sum_i n_i)$, where n_i is the number of Auger counts in the Auger spectrum after background subtraction

and E_i is the corresponding Auger electron energy, and then to normalize the Auger yield to that from Ar. The relative Auger cross sections in this laboratory were then normalized to Stolterfoht's Ar *LMM* Auger cross section⁹ at 0.6 MeV. The mean Auger energies in the present experiment were found to be 72 eV (Si), 94 eV (P), 125 eV (S), 155 eV (Cl), and 185 eV (Ar), with corresponding MCP efficiencies of 54%, 60%, 65%, 68%, and 70%, respectively, as given by Galanti *et al.*²⁰ The normalized Auger yield for Si was then $\text{Eff}(\text{Ar})/\text{Eff}(\text{Si}) = 0.70/0.54 = 1.30$, while those for P, S, and Cl were $0.70/0.60 = 1.17\%$, $0.70/0.65 = 1.08\%$, and $0.70/0.68 = 1.03\%$, respectively. Thus, the MCP detector efficiency corrections were 30% (Si), 17% (P), 8% (S), and 3% (Cl), with a corresponding error assignment to the Auger *LMM* yields of 9% (Si), 5% (P), and 3% (S and Cl) based on the errors in the efficiencies given in Ref. 20.

A flashlight bulb filament biased from 75 to 355 V negative was used as an electron source to test the transmission characteristics of the electrostatic analyzer (ESA). It was found that 30-eV transmission energy was the most efficient for 75- to 200-eV electrons while 60- or 90-eV transmission energy was the most efficient for 250- to 355-eV electrons. It was observed, however, that the number of electrons emitted from the filament depended on the bias voltage that was applied. The Ar *LMM* Auger lines at 203 to 207 eV produced under 1-MeV He^+ ion bombardment provide a constant-number electron source. The geometry of the rectangular gas cell is such that the vertical wall of the cell facing and 1 cm distant from the vertical copper plate at the entrance to the ESA provides an almost perfect plane parallel-plate capacitor. If a positive voltage bias is applied to the gas cell insulated from its surroundings, the electric lines of force will be essentially parallel from the gas cell exit aperture to the ESA entrance aperture at ground potential without alteration of the focusing properties of the ESA. A $\frac{5}{8}$ -in.-thick teflon spacer on the lid of the scattering chamber allowed for the application of a positive bias voltage from 0 to 350 V directly to the gas cell which was thereby electrically insulated from the ESA. The application of the bias voltage provides a retarding voltage to lower the energy of the Auger electrons produced in the gas cell. A calibration curve of relative intensity versus the retarded energy of the Ar *LMM* electrons through the ESA from approximately 50 to 200 eV was obtained by application of $+150$ to 0 V bias to the gas cell. This calibration curve was confirmed and extended to 350 eV by replacement of Ar in the gas cell by nitrogen gas and using the nitrogen *KLL* Auger electrons also produced under 1-MeV He^+ ion bombardment. This calibration curve showed a relative intensity of transmitted electrons monotonically increasing from 27% at 50 eV to 91% at 200 eV to 100% at 350 eV. This calibration curve was then used as an indication of the transmission efficiency of the ESA for the Auger electrons produced in the present experiment. The corrections to the Auger *LMM* cross sections were 81% (Si), 37% (P), 18% (S), 6.3% (Cl), and 0% (Ar) with respective random errors assigned to the corrections of 15% (Si), 8.5% (P), 4.0% (S), 1.5% (Cl), and 0% (Ar).

For the cross-section measurement, it is essential to have an accurate determination of the number of He^+ ions that interact with the target gas atoms. Three tests were made to ensure this determination. One test was to see if the He^+ ion beam current measured at the Faraday cup after passing through the gas cell without gas would change when a positive bias from 0 to 320 V was applied to the Faraday cup. No change in the 100-nA He^+ ion current was observed. The second test involved the measurement of He^+ ion beam current at 0.2-MeV intervals from 0.6 to 2.0 MeV with and without each of the five target gases in the gas cell at 3-mTorr pressure. The current was found to increase in the presence of the gas by 50% for each of the five gases with a random variation of 5% about this value with zero bias on the Faraday cup. This 50% effect remained unchanged for positive biases from 0 to 22.5 V, decreased to 30% at 45 V and 20% at 90 V, and was completely gone for biases greater than 135 V. A head-on collision between the incident He^+ ion and one of the Ar target atoms will produce a recoil Ar ion or atom of several hundred keV, so it is unlikely the additional positive-ion current arises from this recoil effect. A more likely explanation is that the doubly or singly charged ions remaining from the Auger process or from ionization by the He^+ ion beam are swept along by the He^+ beam and are registered on the Faraday cup when little or no positive bias is applied. Once the positive bias on the Faraday cup is sufficiently large (135 V), the residual positive ions are repelled away from the Faraday cup. For all cross-section measurements reported in this experiment, the ion beam current used was that in the absence of the target gas or that with a Faraday cup positive bias greater than 135 V. A third test involves possible incomplete transmission of the He^+ beam through the gas cell in which the particles that enter the cell and strike the back wall of the gas cell would, therefore, not get counted by the Faraday cup. The back rectangular plate on the gas cell is removable and is fixed on the cell with an O ring. The He^+ ion current through the gas cell was measured separately with and without this plate on the cell and revealed an increase of the beam current by 3% when the plate was removed. When a similar test was run with 3-mTorr Ar gas in the cell, a 4% increase in beam current was observed in the absence of the plate. Thus, 4% of the He^+ ion current was lost inside the gas cell during the experiment. This loss in current was accounted for in the determination of the ionization cross sections.

The following procedure was employed to check for possible corrosion or contamination of the ESA and MCP detector, and also to ensure that the MCP efficiency, ESA efficiency, target gas purity, and He ion beam current was not changing throughout the course of the experiment. The Ar *LMM* Auger yield per incident He per target atom was first measured from 0.4- to 2.0-MeV He^+ ion energy. The Ar gas was removed and the scattering chamber was pumped out for several hours. The Si *LMM* Auger yields per incident He^+ ion per target atom was then carefully measured as a function of He^+ ion energy. The silane gas was then pumped out for several hours, and the Ar gas was admitted once again

into the gas cell for 1.2-MeV He^+ ions. A careful check was then made to ensure that the Ar *LMM* Auger value had not changed from its previous value. This procedure was then repeated between every subsequent measurement for P, S, and Cl, and the range of variation was found to be from -3% to 6% of the Ar values given in this paper. It should also be mentioned that the Ar, S, and P measurements were repeated twice at all He^+ ion bombarding energies, while the Si and Cl measurements were repeated three times at all energies.

Target gas purity was checked primarily with the RGA. An independent check for the presence of nitrogen (or atmospheric) leaks in the gas supply transport system was made by changing the sweep voltage range on the ESA from -280 to -390 V. It was found that if a nitrogen contamination of 10% or greater was present, the nitrogen *KLL* Auger electrons would appear in the spectrum. This test for possible nitrogen contamination was also made at 1.2-MeV He^+ ion bombardment between each series of data collection for each target gas, namely, the same time the argon test was made. No evidence of any nitrogen contamination was found throughout the course of the entire experiment. The test of contamination by the RGA, however, gives a more accurate measurement (better than 1% error) of nitrogen contamination.

The relative errors in the experiment came from essentially six sources: (1) background subtraction of the Auger spectra (error estimated to be $\sim 10\%$); (2) gas-pressure measurement (error $\sim 5\%$); (3) beam-current measurement in Faraday cup ($\sim 5\%$); (4) MCP efficiency calibration (1%–9%); (5) ESA efficiency calibration (0%–15%); and (6) atmospheric contamination of target gas ($\sim 1\%$). These random errors combine quadratically to give a random error assignment of 22% (Si), 16% (P), 13% (S), and 12% (Cl and Ar).

In Sec. III the subject of isotropy of the Auger electron emission will be discussed, where it is pointed out that some evidence exists for a forward preponderance of Auger electron emission by as much as 10%, while other evidence exists for no anisotropy. A 10% departure from isotropy would mean that the experimental cross sections in this experiment would be systematically too low by as much as 10%.

Finally, all *LMM* Auger electron yields were normalized to the Ar yield, which in turn was normalized to Stolterfoht's value⁹ for Ar at 0.6 MeV, to which he assigned a 16% error. Thus, our relative error of 12–22% will be compounded together with Stolterfoht's error assignment of 16%. At the beginning and end of collection of all the experimental data given in this paper, a measurement was made of the carbon *KLL* Auger yield in CH_4 and the nitrogen *KLL* Auger yield, both at 0.6 MeV, and the measurements in this laboratory agreed completely with the values Stolterfoht obtained⁸ in a separate experiment. This agreement confirms the reliability of the normalization procedure used in this experiment.

III. RESULTS

Typical *LMM* Auger electron spectra of Si, P, S, Cl, and Ar, produced by 1.2-MeV He^+ ion bombardment of

SiH_4 , PH_3 , H_2S , CH_3Cl , and Ar, respectively, are given in Fig. 1. These Auger spectra are superimposed on the continuous background of electrons resulting from binary ion-electron collisions. The Auger yield for a given spectrum is obtained by subtracting this secondary-electron background which has been fitted first by a second-, third-, or fourth-degree polynomial as is explained in the next paragraph. The Auger spectra obtained after the background has been subtracted are also given in Fig. 1.

It is mentioned in Ref. 18 that a major difficulty in obtaining an Auger yield is the determination of the shape of the secondary-electron background spectrum. The procedure followed in this experiment is to obtain the experimental spectrum about 15–25 eV beyond the lower-energy limit and upper-energy limit of the observed Auger peak itself. For example, the Si $L_{23}MM$ Auger peak occurs²³ in the energy range 52–105 eV, but the Si $L_{23}MM$ Auger spectrum from SiH_4 in the present experiment was collected from 35 to 130 eV. The shape of the secondary electron background was determined from the experimental points between 35–52 eV and between 105–130 eV and then fitted by a fourth degree polynomi-

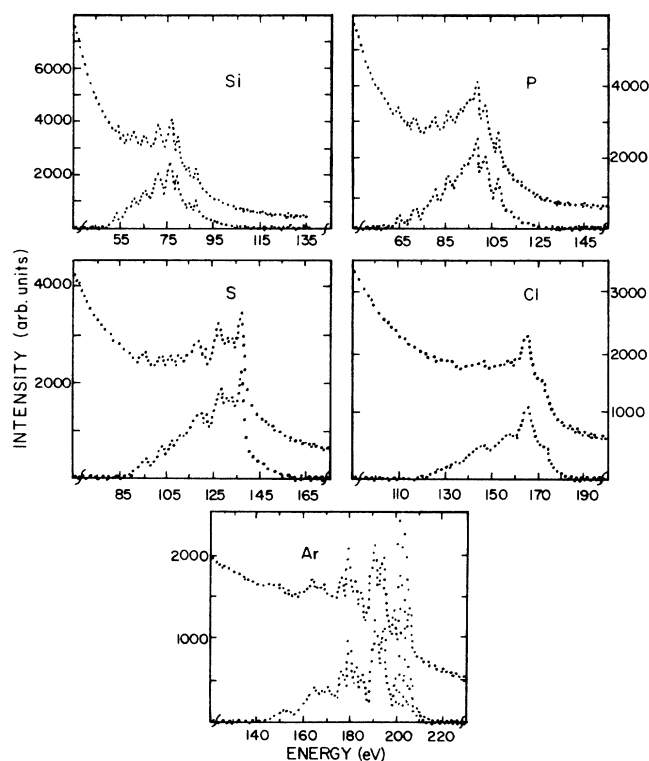


FIG. 1. LMM Auger-electron spectra of Si, P, S, Cl, and Ar as a function of Auger-electron energy in eV. The spectra are produced by 1.2-MeV He^+ ion bombardment of SiH_4 , PH_3 , H_2S , CH_3Cl , and Ar, respectively, and reveal some of the individual line structure in each case. The top curve is the spectrum including the background, while the lower curve gives the Auger spectrum after the background has been subtracted. The vertical scale in each case represents the number of Auger electrons recorded in arbitrary units.

al. Fourth-degree polynomials were also used for the PH_3 background spectra, while a third-degree polynomial was used for the H_2S and CH_3Cl background, and either a second- or third-degree polynomial for the Ar background.

The Auger electron yields were then found by integrating the spectrum after the background had been subtracted. These Auger electron yields were then converted to total Auger cross sections under the assumption that the Auger electron emission is isotropic, as has been assumed also by several other authors.^{9,24,25} Kobayashi *et al.*²⁶ found the KLL Auger electron emission from carbon and nitrogen under 2.0-MeV proton and 2.5-MeV He^+ ion bombardment to be isotropic. On the other hand, Cleff and Mehlhorn²⁷ found experimental evidence that LMM Auger electron emission from Ar was nonisotropic to about 10% under electron bombardment. Later, Stolterfoht *et al.*⁹ reported that the LMM Auger electron emission produced under 100- to 300-keV proton bombardment of Ar was isotropic within their experimental error of about 10%. In principle, the isotropic Auger electron emission following an L -shell vacancy might not be true. However, the largest reported nonisotropic LMM Auger electron emission is about 10%, which is less than the experimental errors of 12–22% given in this experiment. One should not expect an anisotropy greater than 10% for the Auger electrons in this experiment because the elements Si, P, and S all have the same number (18) of electrons as Ar, respectively, in the target molecules SiH_4 , PH_3 , and H_2S . Thus, we have assumed isotropy for the emission of all LMM Auger electrons in the present experiment. Since the electrons were detected at 90° to the primary He^+ beam direction, a departure from isotropy would imply a correspondingly lower experimental Auger cross section.

The Auger spectra given in Fig. 1 come mainly from L_2MM or L_3MM Auger transitions because the Coster-Kronig transitions (L_1 vacancy is immediately filled with an electron either from the L_2 or L_3 shell) convert most of the L_1 vacancies into L_2 or L_3 vacancies.¹² McGuire¹² has calculated the Coster-Kronig yields of the L_1 shell to be 0.97 and the L_1MM Auger yields to be ≈ 0.03 for the series of elements Si, P, S, Cl, and Ar. According to the same calculations, the L_1 -, L_2 -, and L_3 -shell fluorescence yields and L_2 -shell Coster-Kronig yields are negligible. If the fluorescence yield, Auger yield, and Coster-Kronig yield of the L_i th shell are labeled, respectively, as ω_i , a_i , and $\sum_{j>i} f_{ij}$, then

$$a_i + \omega_i + \sum_{j>i} f_{ij} = 1$$

and the total ionization cross section σ_L is then given by

$$\begin{aligned} \sigma_L &= \sigma_{L_1} + \sigma_{L_2} + \sigma_{L_3} \\ &= (a_1 + \omega_1 + f_{12} + f_{13})\sigma_{L_1} \\ &\quad + (a_2 + \omega_2 + f_{23})\sigma_{L_2} + (a_3 + \omega_3)\sigma_{L_3} . \end{aligned}$$

Since $\omega_1 \approx \omega_2 \approx \omega_3 \approx 0$, $a_1 \approx 0$, and $f_{23} \approx 0$, we get

$$\sigma_L = (f_{12} + f_{13})\sigma_{L_1} + a_2\sigma_{L_2} + a_3\sigma_{L_3} .$$

TABLE I. *L*-shell ionization cross sections of Si, P, S, Cl, and Ar obtained, respectively, by He⁺ ion bombardment of SiH₄, PH₃, H₂S, CH₃Cl, and Ar gases. The errors are random probable errors as discussed at the end of Sec. II.

He ⁺ ion energy (MeV)	<i>E</i> / <i>A</i> (MeV/amu)	Si cross section (10 ⁻¹⁷ cm ²)	P cross section (10 ⁻¹⁷ cm ²)	S cross section (10 ⁻¹⁷ cm ²)	Cl cross section (10 ⁻¹⁷ cm ²)	Ar cross section (10 ⁻¹⁷ cm ²)
0.4	0.100		2.75±0.56			
0.5	0.125	5.41±1.12	3.39±0.70			
0.6	0.150	5.57±1.18	3.97±0.67	1.11±0.15	0.55±0.19	0.49±0.06
0.7	0.175	6.19±1.31	4.13±0.66	1.53±0.24	0.67±0.10	
0.8	0.200	6.20±1.31	4.17±0.78	1.89±0.29	0.87±0.16	0.74±0.07
1.0	0.250	6.28±1.29	4.41±0.71	1.96±0.28	1.02±0.20	0.86±0.09
1.2	0.300	6.14±1.41	4.15±0.73	2.18±0.32	1.28±0.22	1.09±0.17
1.4	0.350	5.70±1.25	3.93±0.69	2.22±0.31	1.36±0.22	1.14±0.11
1.6	0.400	5.25±1.19	4.13±0.75	2.50±0.33	1.39±0.23	1.20±0.19
1.8	0.450	5.50±1.15	3.64±0.62	2.38±0.35	1.60±0.22	1.35±0.17
1.9	0.475		3.85±0.63			
2.0	0.500	3.96±0.88		2.48±0.33	1.63±0.21	1.30±0.20
2.1	0.525	3.60±0.82	3.22±0.65			

On the other hand, the experimental Auger cross sections σ_A^{expt} is

$$\sigma_A^{\text{expt}} = (a_2 f_{12} + a_3 f_{13}) \sigma_{L_1} + a_2 \sigma_{L_2} + a_3 \sigma_{L_3}.$$

Therefore, since $a_2 \approx a_3 \approx 1$, then

$$\sigma_A^{\text{expt}} = \sigma_L.$$

Thus, the integrated area of the L_2MM and L_3MM Auger spectra may be used to obtain the total *L*-shell ion-

ization cross section σ_L for the formation of the vacancies in the L_1 , L_2 , and L_3 shells.

The experimental *L*-shell ionization cross sections for Si, P, S, Cl, and Ar as a function of He⁺ ion bombarding energies are given in Table I. The variation of the *L*-shell ionization cross section as a function of projectile energy per amu is given in Figs. 2–6, respectively, for Ar, Cl, S, P, and Si. Theoretical predictions by Lapicki²⁸ of these *L*-shell ionization cross sections, both for the ECPSSR

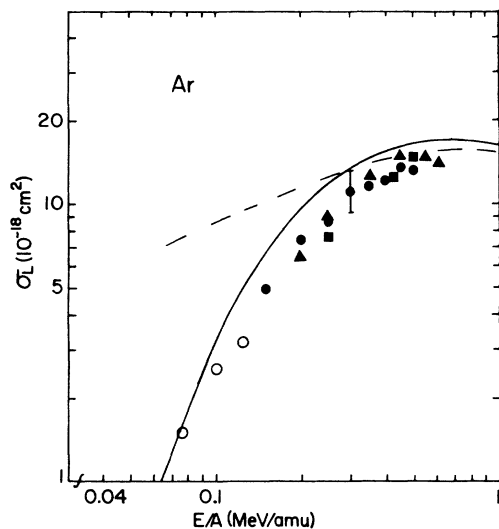


FIG. 2. *L*-shell ionization cross section in 10⁻¹⁸ cm² in Ar for He⁺ ions in MeV/amu units. The solid and dashed curves are, respectively, the ECPSSR and PWBAR theories calculated by Lapicki (Ref. 28). The open circles are the experimental measurements by Stolterfoht *et al.* (Ref. 9), the solid triangles are the measurements of Maeda *et al.* (Ref. 13), the solid squares are by Watson and Toburen (Ref. 7), and the solid circles are the present experimental measurements. The experimental measurements are in fair agreement with the ECPSSR theory.

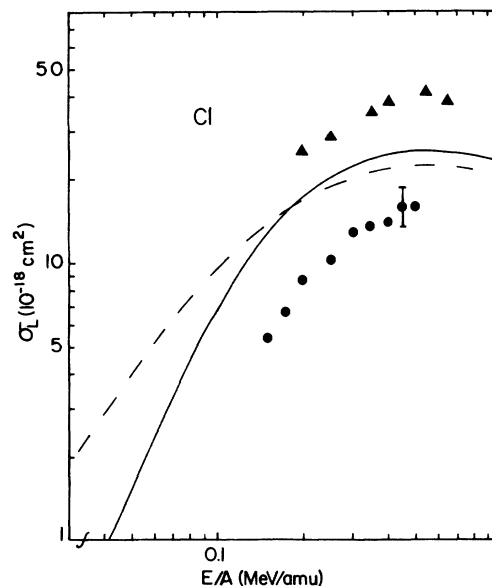


FIG. 3. *L*-shell ionization cross section in 10⁻¹⁸ cm² in Cl for He⁺ ions in MeV/amu units. The solid and dashed curves are, respectively, the ECPSSR and PWBAR theories calculated by Lapicki (Ref. 28). The closed triangles are experimental measurements by Maeda *et al.* (Ref. 13) for He⁺ ions in gaseous CCl₂F₂, and are systematically higher than the theories, while the closed circles are the present experimental measurements for He⁺ ions in gaseous CH₃Cl, and are systematically lower than the theories.

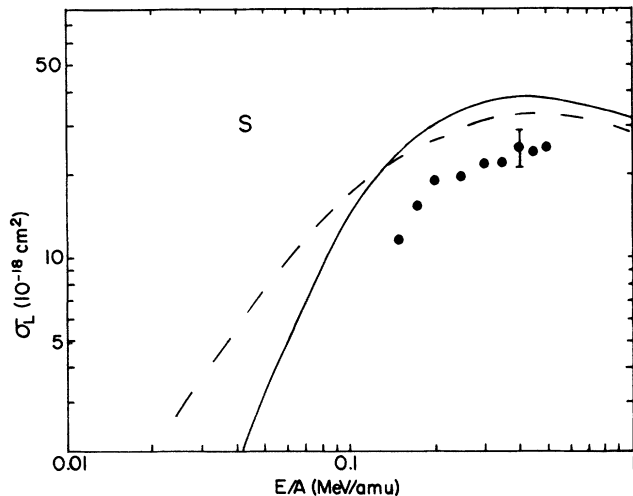


FIG. 4. L -shell ionization cross section in 10^{-18} cm^2 in S for He^+ ions in MeV/amu units. The solid and dashed curves are, respectively, the ECPSSR and PWBAR theories calculated by Lapicki (Ref. 28). The closed circles are the present experimental measurements made for S in H_2S gas.

and PWBAR theories, are also given on the figures along with experimental cross sections for Ar and Cl produced at other laboratories.

In Fig. 7 the experimental cross sections are scaled according to the BEA universal curve²⁹ $U_L^2 \sigma_L / Z_1^2$ as a function of $E_{\text{He}^+} / \lambda U_L$, where U_L is the binding energy of the L -shell electron (we used the values given by the de Alti and Decleva³⁰). σ_L is the measured ionization cross section, Z_1 is the atomic number of the projectile, E is the energy of the He ion, and λ is the ratio of the He-ion mass to that of the electron. The purpose of the scaling is to examine the target-atom Z_2 dependence of the L -shell ionization cross sections. The solid curve in the figure is the BEA theoretical dependence given by Hansen.²⁹

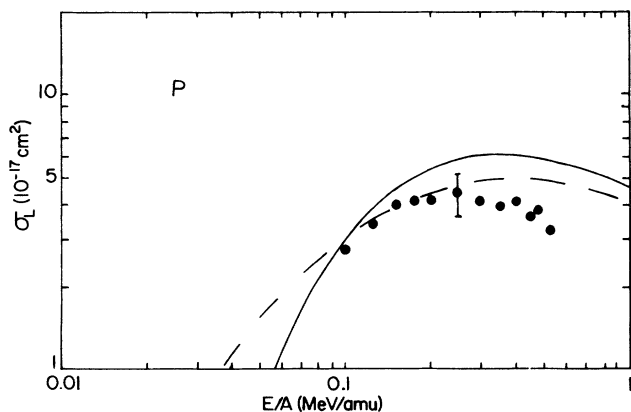


FIG. 5. Same as Fig. 4 except for P and that the cross sections is in 10^{-17} cm^2 and that the experimental measurements for P are made in PH_3 gas.

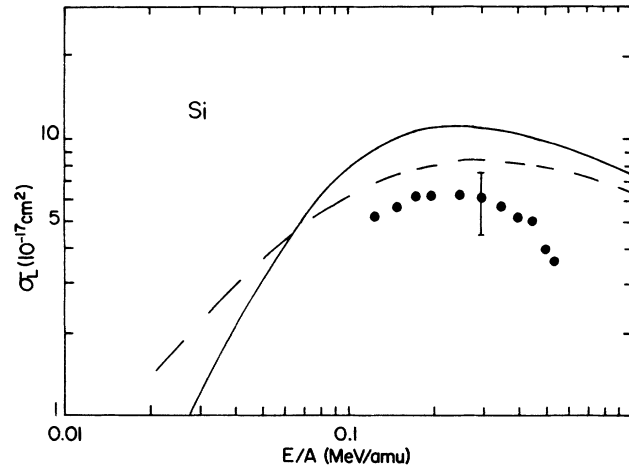


FIG. 6. Same as Fig. 5 for Si and that the experimental measurements for Si are made in SiH_4 gas.

IV. DISCUSSION

It is seen from Fig. 2, that within experimental error, the experimental L -shell ionization cross sections of Ar produced in this laboratory are in good agreement with those measured by Watson and Toburen⁷ and by Maeda *et al.*¹³ They are also in fair agreement with the ECPSSR theory for the entire energy range given in the figure. In contrast, the experimental cross sections of Ar deviate considerably from the PWBAR predictions at lower He^+ ion bombarding energies [$0.07 \leq E_{\text{He}^+} / A$ (MeV/amu) ≤ 0.15].

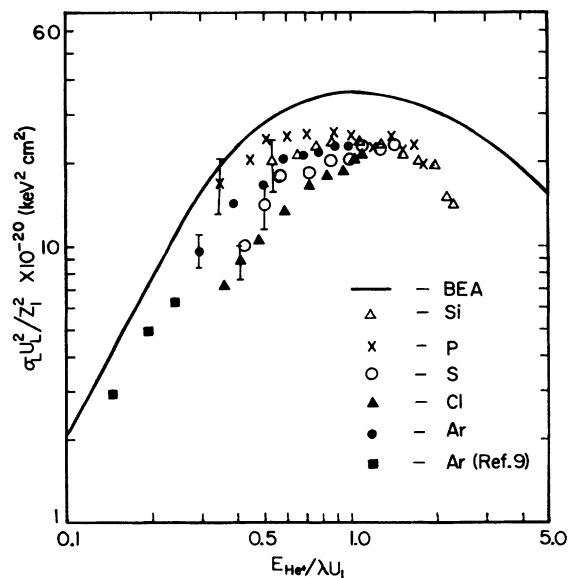


FIG. 7. Experimental L -shell ionization cross sections of Si, P, S, Cl, and Ar scaled according to BEA theory. The solid curve represents the BEA predictions by Hansen (Ref. 29) and the solid squares are the experimental measurements of He in Ar by Stolterfoht *et al.* (Ref. 9).

The experimental Ar *L*-shell ionization cross sections by Watson and Toburen⁷ and by Maeda *et al.*¹³ are for doubly charged He²⁺, while the Ar measurements in this laboratory and those of Stolterfoht⁹ at 600 keV are for singly ionized He⁺. One might have *a priori* anticipated a lower *L*-shell ionization cross section for the singly charged ions than for the doubly charged ions because the bound electron in He⁺ would screen the He nuclear charge. The results in Fig. 2, however, indicate good agreement between the singly and doubly charged He measurements. A similar behavior occurred between singly and doubly charged 600-keV He ions in *K*-shell ionization of carbons in CH₄ and C₂H₆ measured, respectively, by Stolterfoht⁸ and by Watson and Toburen.⁷ An explanation for this is as follows. First, the He ion, whether singly or doubly charged, must be sufficiently energetic to penetrate the Ar *L*-shell or the C *K*-shell target atom. 0.6- to 2.0-MeV He ions are easily able to do this because their velocities are of the same magnitude as the C *K*-shell ionization energy (290 eV) and Ar *L*-shell ionization energy (265 eV). The radius of a He⁺ ion is 2.65×10^{-11} m, while the Herman and Skillman³¹ radius of the Ar *L* shell is 1.54×10^{-11} m and that of the C *K* shell is 0.734×10^{-11} m, with corresponding areas, respectively, of 22.1×10^{-22} m², 7.45×10^{-22} m², and 1.69×10^{-22} m². Thus, the effective area of the He⁺ ion is three times larger than that of the Ar *L* shell and 13 times larger than that of the C *K* shell. What this means is that the Ar *L* shell and C *K* shell will see essentially the doubly charged nucleus of the penetrating He ion, thereby resulting in an Ar *L*-shell and C *K*-shell ionization cross section that is the same for both doubly and singly charged He ions at these MeV energies.

It is surprising that the experimental *L*-shell ionization cross sections for Cl (Fig. 3) produced in this laboratory are nearly 2.5 times lower than the experimental values given by Maeda *et al.*,¹³ but are only about 40% lower than the ECPSSR theoretical predictions and about 30% lower than the PWBAR predictions at higher He⁺ ion bombarding energies. The values of Maeda *et al.*¹³ are about 60% higher than the same theoretical predictions and have errors of about 50% which are over twice the errors we have in the present measurements. They also used the gas molecule CCl₂F₂, which are more screening and chemical-binding effects for Cl *LMM* Auger electron emission than would be expected from the gaseous methyl chloride CH₃Cl employed in the present experiment. Nevertheless, we measured the Cl *LMM* Auger yield from CCl₂F₂ under 1.2-MeV He⁺ ion bombardment and found that the Cl *L*-shell ionization cross sections from CCl₂F₂ and CH₃Cl are the same within experimental error. We do not believe the difference could be caused by the fact that they used doubly charged He²⁺ ions while we used singly charged He⁺ ions, because our calculations for Cl based on considerations given in the previous paragraph indicate that at MeV He energies the charge state of the He ion does not affect the *L*-shell ionization cross sections. We do not know why their values are so high, but would like to emphasize that our *L*-shell ionization cross sections for Cl follow the general trend predicted by the ECPSSR theory but deviate from the

PWBAR theory at lower He⁺ ion energies.

From Fig. 4 it is seen that the experimental *L*-shell ionization cross sections of S are about 34% below the ECPSSR theoretical values and about 30% below the PWBAR theory at higher He⁺ energies. At lower He⁺ ion bombarding energies the experimental cross sections deviate to a greater extent from the PWBAR values. Both S and Cl *L*-shell ionization cross sections follow the general trend of the ECPSSR theory for the energy-mass range from 0.1 to 0.5 MeV/amu.

At lower He⁺ ion bombarding energies, the experimental *L*-shell ionization cross sections of P have closer agreement to both ECPSSR and PWBAR theories. At higher He⁺ energies, however, these cross sections deviate from both theories by 45% (ECPSSR) to 33% (PWBAR). From Fig. 6 it is seen that the experimental *L*-shell ionization cross sections of Si are about 43% and 62% lower than the ECPSSR theoretical value and about 25% to 53% lower than the PWBAR predictions, with the largest deviation occurring at the higher energies. Since the He⁺ ion energy range in this study covers only the peak region of the P and Si ionization cross-section curves, it is difficult to make any conclusion about the general trend of the experimental curves for P and Si. As can be seen from Figs. 5 and 6, however, the experimental ionization cross sections of P and Si fall off more rapidly at higher He⁺ ion bombarding energy than the theoretical predictions of both ECPSSR and PWBAR theories. The *L*-shell ionization cross sections of Ar for H⁺ ion bombardment near and into the peak region of the cross section curve measured by Maeda *et al.*¹³ are seen in Ref. 1 also to fall off more rapidly than the ECPSSR predictions. Our recent preliminary measurements of the Ar and Si *L*-shell ionization cross sections produced by 0.4- to 2.0-MeV proton bombardment also show this rapid fall in cross section over the peak region of the cross section curve.

In Fig. 7, in which the experimental measurements are scaled according to the BEA predictions of Hansen,²⁹ all measurements are from 17% to 64% below the theory. For the region from $0.7 < E_{\text{He}^+} / \lambda U_L < 1.75$, the experimental *L*-shell ionization cross sections for all five elements fall upon a single curve within experimental error, but generally about 37% below the BEA formalism. Thus, no *Z*₂ dependence seems to exist in this region. For $E_{\text{He}^+} / \lambda U_L < 0.7$, the Si, P, and Ar values follow the general BEA trend, but the S and Cl values fall off more rapidly, thereby indicating a possible *Z*₂ effect. Such an effect, however, is puzzling since S and Cl are adjacent in the Periodic Table, and one might have expected the Ar values to be closer to S and Cl than to Si and P.

One should not expect to obtain a pure atomic cross section from an atom in a molecular environment because of possible molecular effects. In a target molecule, the outer-shell electrons of the target atom are bound to the secondary atoms in the molecule thereby reducing the probability of ejection of the Auger electrons. For the hydrogen-containing molecules involved in this experiment, one might anticipate not-too-large an effect from chemical binding because of the intermediate electronegativity of hydrogen.³² We have previously studied¹⁸

molecular effects in carbon *KLL* Auger emission in a series of carbon-containing molecules where we found 32% less carbon Auger-electron production in CF_4 than in CH_4 , and interpreted the results in terms of inelastic scattering of the Auger electrons by the secondary atoms in the molecule. A calculation based on the approach used there gives an estimate of molecular effects to be 4%, 5%, 6%, and 10%, respectively, for H_2S , PH_3 , SiH_4 , and CH_3Cl . The calculation involves the use of covalent atomic radii and interatomic distances tabulated in Ref. 33. These estimated molecular effects would seem reasonable based upon an increasing value for greater hydrogen (and Cl) content in the molecule.

As explained earlier, our experimental *L*-shell ionization cross sections are made relative to the experimental *L*-shell ionization cross section of Ar at 600-keV He^+ ion bombardment by Stolterfoht *et al.*⁹ This reference cross section is 25% below the ECPSSR theoretical prediction. If the Ar cross section at 600-keV He^+ ion energy agreed completely with the ECPSSR theory, the cross sections reported in this article would be only 20% or less below

the ECPSSR theory.

In conclusion, the experimental *L*-shell ionization cross sections of Cl, S, P, and Si in the molecules CH_3Cl , H_2S , PH_3 , and SiH_4 , respectively, are 30% to 60% lower than the ECPSSR theoretical predictions, while the *L*-shell ionization cross sections of Ar are close to the ECPSSR theoretical prediction roughly within the experimental error. We have discussed molecular effects and possible anisotropic Auger emission that could cause a lower *L*-shell ionization cross section than the theory for Cl, S, P, and Si.

ACKNOWLEDGMENTS

The authors are grateful to the Baylor University Research Committee and to the Department of Physics for assistance in carrying out the work reported in this paper. We also wish to thank Professor Gregory Lapicki who is very helpful in providing his theoretical calculations.

-
- ¹W. Brandt and G. Lapicki, *Phys. Rev. A* **20**, 465 (1979).
²W. Brandt and G. Lapicki, *Phys. Rev. A* **23**, 1717 (1981).
³H. Paul, *IEEE Trans. Nucl. Sci.* **NS-28**, 1119 (1981).
⁴H. Paul and J. Muhr, *Phys. Rep.* **135**, 47 (1986).
⁵H. Paul, *Nucl. Instrum. Methods B* **4**, 211 (1984).
⁶W. Brandt and G. Lapicki, *Phys. Rev. A* **10**, 474 (1974).
⁷R. L. Watson and L. H. Toburen, *Phys. Rev. A* **7**, 1853 (1973).
⁸N. Stolterfoht, D. Schneider, and K. G. Harrison, *Phys. Rev. A* **8**, 2363 (1973).
⁹N. Stolterfoht, D. Schneider, and P. Ziem, *Phys. Rev. A* **10**, 81 (1974).
¹⁰N. Kobayashi, N. Maeda, H. Hori, and M. Sakisaka, *J. Phys. Soc. Jpn.* **40**, 1421 (1976).
¹¹H. Kojima, N. Kobayashi, N. Maeda, and M. Sakisaka, *J. Phys. Soc. Jpn.* **46**, 198 (1979).
¹²E. J. McGuire, *Phys. Rev. A* **3**, 587 (1971).
¹³N. Maeda, N. Kobayashi, H. Hori, and M. Sakisaka, *J. Phys. Soc. Jpn.* **40**, 1430 (1976).
¹⁴D. J. Volz and M. E. Rudd, *Phys. Rev. A* **2**, 1395 (1970); J. B. Crooks and M. E. Rudd, *ibid.* **3**, 1628 (1971); M. E. Rudd, *ibid.* **10**, 518 (1974).
¹⁵L. H. Toburen, W. E. Wilson, and L. E. Porter, *J. Chem. Phys.* **67**, 4212 (1977).
¹⁶C. Benazeth, N. Benazeth, and L. Viel, *Suf. Sci.* **65**, 165 (1977).
¹⁷E. Gerjuoy, *Phys. Rev.* **148**, 54 (1966).
¹⁸R. D. McElroy, Jr., W. M. Ariyasinghe, and D. Powers, *Phys. Rev. A* **36**, 3674 (1987).
¹⁹W. M. Ariyasinghe, R. D. McElroy, Jr., and D. Powers, *Nucl. Instrum. Methods B* **24/25**, 162 (1987).
²⁰M. Galanti, R. Gott, and J. F. Renaud, *Rev. Sci. Instrum.* **42**, 1818 (1971).
²¹J. P. Macau, J. Jamar, and S. Gardier, *IEEE Trans. Nucl. Sci.* **NS-23**, 2049 (1976).
²²N. Stolterfoht and D. Schneider, *Phys. Rev. Lett.* **11**, 721 (1974).
²³F. Maracci, R. Platania, and R. Salomone, *J. Electron. Spectrosc. Relat. Phenom.* **19**, 155 (1980).
²⁴L. H. Toburen, *Phys. Rev. A* **5**, 2482 (1972).
²⁵D. L. Matthews and F. Hopkins, *Phys. Rev. Lett.* **40**, 1326 (1978).
²⁶N. Kobayashi, T. Irie, N. Maeda, H. Kojima, S. Akanuma, and M. Sakisaka, *J. Phys. Soc. Jpn.* **47**, 234 (1979).
²⁷B. Cleff and W. Mehlhorn, *Phys. Lett.* **37A**, 3 (1971).
²⁸G. Lapicki (private communication).
²⁹L. S. Hansen, *Phys. Rev. A* **8**, 822 (1973).
³⁰G. de Alti and P. Decleva, *Chem. Phys. Lett.* **45**, 103 (1977).
³¹F. Herman and S. Skillman, *Atomic Structure Calculations* (Prentice-Hall, Englewood Cliffs, NJ, 1963).
³²R. T. Sanderson, *Chemical Periodicity* (Reinhold, New York, 1960), p. 167.
³³*CRC Handbook of Chemistry and Physics*, edited by R. C. Weast, M. H. Astle, and W. H. Beyer, 67th ed. (CRC, Boca Raton, Florida, 1987), pp. F-158-162.